Journal of Bioresources and Bioproducts 9 (2024) 174–184

Contents lists available at ScienceDirect

Journal of Bioresources and Bioproducts

journal homepage: https://www.keaipublishing.com/en/journals/journal-of-bioresources-and-bioproducts/

Research Article

Production of chitosan-based composite film reinforced with lignin-rich lignocellulose nanofibers from rice husk

Hye Jee Kang[a], Yeon Ju Lee[a], Jin Kyoung Lee[b], Irnia Nurika[c], Sri Suhartini[c], Deokyeong Choe[a], Dong Hyun Kim[a], Hoon Choi[d], Natasha P. Murphy[d], Ho Yong Kim[e], Young Hoon Jung[a,*]

[a] School of Food Science and Biotechnology, Kyungpook National University, Daegu 41566, Republic of Korea
[b] CPR S&T Co., Ltd., Gunpo 15880, Republic of Korea
[c] Department of Agroindustrial Technology, Faculty of Agricultural Technology, Universitas Brawijaya, Malang 65145, Indonesia
[d] Renewable Resources and Enabling Sciences Center, National Renewable Energy Laboratory, Golden, CO 80401, United States
[e] Center for Bio-based Chemistry, Korea Research Institute of Chemical Technology, Ulsan 44429, Republic of Korea

ARTICLE INFO

Keywords:
Rice husk
Lignocellulose nanofiber
Lignin-based material
Chitosan film
Upcycling

ABSTRACT

Lignocellulosic nanofibers (LCNFs), implying lignin-containing cellulose fibers, maintain the properties of both lignin and cellulose, which are hydrophobic and hydrophilic, respectively. The presence of hydrophobic lignin in LCNFs is expected to be an economical and attractive option that can improve the thermal and mechanical properties of polymers. Thus, this study was conducted to produce lignin-rich LCNFs from sugar-rich waste obtained from rice husks after acidic pretreatment. The LCNFs were produced from the lignin-rich solid fractions obtained after pretreatment and enzymatic hydrolysis, which were then incorporated as an additive into a chitosan-based film. The variations in lignin content in the range of approximately 50.6%–66.8% in differently obtained LCNFs gave significantly different optical strengths and mechanical properties. These controllable processes may allow for customized film formation. Additionally, the glucose-rich liquid fractions obtained after pretreatment and enzymatic hydrolysis were used as a substrate for ethanol fermentation to achieve total utilization of rice husk biomass waste. In conclusion, the lignin-rich biomass fraction holds promise as a suitable material for chitosan-LCNF film and has the potential to increase the economic feasibility of the biomaterial industry.

1. Introduction

Rice husk, the hard protective layer that envelops the inner grain of rice, constitutes approximately 20%–25% of the entire rice structure. With rice consumption being a staple for about 755 million metric tons (Shaheen et al., 2022), an estimated 170 million tons of rice husks are generated as a byproduct. Rice husks also contain useful components, including cellulose (35%), hemicellulose (25%), lignin (20%), and silica (20%) (Ma'ruf et al., 2017). Nevertheless, the utilization of rice husk has been relatively limited, primarily for feed sources (Chieng and Kuan, 2022) or biochemical production (Banerjee et al., 2009; Dagnino et al., 2017).

Lignocellulose, such as rice husk, is the most abundant substrate (Howard et al., 2003). It holds great promise as a valuable resource in biorefinery applications (Walls and Rios-Solis, 2020). The concept of biorefinery, as defined by the International Energy Agency (Cherubini, 2010), centers around "the sustainable processing of biomass into a spectrum of marketable products." Sustainability is the underlying motivation behind the exploration of lignocellulosic biomass deconstruction for circular-loop bioindustry. These

* Corresponding author.
E-mail address: younghoonjung@knu.ac.kr (Y.H. Jung).

https://doi.org/10.1016/j.jobab.2024.03.002

Available online 15 March 2024

strategies include the conversion of sugar into useful chemicals through pretreatment, saccharification, and fermentation (including metabolic engineering) approaches as well as the direct extraction and valorization of polymeric compounds such as cellulose and lignin (Rodionova et al., 2022).

Nano/microfibrillated cellulose (N/MFC), a promising alternative material from the lignocellulosic structure, has shown remarkable properties including biodegradability, high surface area, excellent mechanical strength, flexibility, mixability, and high elasticity (Jang et al., 2021; 2023). However, the production of lignin-containing nanofibrillated cellulose (lignocellulose nanofiber) involves the inclusion of portions of hemicellulose and lignin, resulting in higher production efficiency and lower energy consumption (Jiang et al., 2018). The utilization of lignocellulose nanofibers (LCNFs) is an attractive option for modifying the surface properties of N/MFC without an additional chemical-driven modification (i.e., more environmentally friendly) process. Compared with N/MFC, LCNF can be obtained using more environmentally friendly processes, while maintaining the properties of both lignin and N/MFC, such as high thermal stability, hydrophobicity, and low polarity (Bian et al., 2017; Yousefhashemi et al., 2019).

Previous studies have confirmed the positive effect of adding N/MFC as a reinforcing agent on chitosan films. For instance, Fernandes et al. (2010) reported that the composite of chitosan-NFC exhibits superior dispersion in their matrix and homogeneous, flexible, better thermomechanical properties. Another study reported that NFC exerted the effect of suppressing the water uptake of chitosan (Supanakorn et al., 2021). Nevertheless, because of its highly hydrophilic nature, additional hydrophobicity might be required during the preparation of chitosan-based composites. The presence of hydrophobic lignin in LCNFs may be an economical and attractive option for reducing the water absorption of composites and improving the thermal and mechanical barrier properties of polymers. However, there is limited data concerning LCNFs with different amounts of lignin as a reinforcing agent on the chitosan matrix.

Meanwhile, many studies carried out ethanol production through a multi-process containing chemical pretreatment, enzymatic hydrolysis, and fermentation. Few studies have discussed the residual solids even though that process leaves residual solids rich in structural carbohydrates. Zhu et al. (2011) have conducted a study of the integrated production of cellulosic biofuel (ethanol) and nano-fibrillated cellulose (NFC) by enzymatic fractionation, showing the production possibility of NFC from the solid fraction obtained from saccharification. Therefore, we conducted this study, following a simple ethanol production process flow to explore the possibility of using the remaining solids as LCNFs and preparing LCNFs with various lignin contents by adjusting the acid pretreatment time. We applied diluted acid pretreatment and enzymatic hydrolysis, which are widely used due to their low cost and simplicity, to produce bioethanol from rice husk. Next, using the solid fraction remaining after enzymatic hydrolysis, we investigated its applicability as a material for LCNFs production. Furthermore, we demonstrate a simple method to use LCNFs for potentially reinforcing the chitosan polymer or selectively adjusting its characteristics as a case study.

2. Materials and methods

2.1. Rice husk and its compositional analysis

Dried and milled rice husks (50–100 mesh (100–270 μm) passed) were obtained from Saron Filler (Anseong, Gyeonggi-do, Korea); and their compositions were analyzed according to the Laboratory Analytical Procedures of the National Renewable Energy Laboratory (NREL; NREL/TP-510–42618 and 42623). Sugars were quantified using high-performance liquid chromatography (HPLC; LC-6000, Futecs, Daejeon, Korea) equipped with a refractive index detector (RID; RI-6000, Futecs) and a Shodex SP0810 column (Showa Denko, Kawasaki, Japan). Sugar derivatives, including alcohols, aldehydes, and organic acids, were analyzed on an HPLC-RID equipped with an Aminex HPX-87H column (Bio-Rad, Hercules, CA, USA).

2.2. Chemical pretreatment, enzymatic hydrolysis, and fermentation

The rice husks were chemically pretreated with 1% (*w/V*) sulfuric acid at 15% (*w/V*) solids loading in a microwave digestion system (MARS 6, CEM Corporation, Matthews, NC, USA) at 190°C (at 5 min ramping) with 5–60 min holding at 1 800 W. The pretreated slurry was filtered through Miracloth (EMD Millipore Corporation, Billerica, MA, USA) to separate the solid and liquid fractions. Next, the solid fraction was washed with distilled water until the pH reached 7 to eliminate any residual sulfuric acid. Some portions were dried at 45°C for 3 d for compositional analysis, and others were stored at 4°C for further processes.

The rice husks were enzymatically hydrolyzed with 20 filter paper units (FPU) of the commercial enzyme Cellic CTec2 (218 FPU/mL, measured value; Novozymes, Copenhagen, Denmark) per gram substrate. Ten percent of the solids were incubated in sodium citrate buffer (0.05 mol/L, pH 4.8) for 48 h at 50°C and 250 r/min in a shaking incubator (BF-50SIR, Biofree, Seoul, Korea). The hydrolysates were filtered through Miracloth to separate the solid and liquid fractions. The remaining solids were rinsed with distilled water before the resulting solid slurry was stored at 4°C for LCNFs production, and a portion was dried at 40°C for 3 d for compositional analysis.

The liquid fraction (i.e., main sugar fraction) was used as a substrate for *Saccharomyces cerevisiae* to produce bioethanol as a conceptual study to demonstrate the possibilities of rice husk-derived biorefinery. Fermentation was performed by referring to and modifying a previous study (Ranatunga et al., 1997). The liquor of pretreated and enzymatically hydrolyzed rice husks was fermented in a sterilized medium containing 1% (*w/V*) yeast extract (Y) and 2% (*w/V*) peptone (P). A culture of 5% *S. cerevisiae* D_5A, grown in a yeast peptone (YP) medium containing 5% (*w/V*) glucose in a shaking incubator at 37°C with stirring at 150 r/min for 12 h, was used for ethanol production at 37°C with stirring at 150 r/min for 48 h. The ethanol yield was determined as a percentage of

the theoretical maximum yield of glucose (i.e., the produced amount (g) of ethanol / (0.51 × the consumed amount (g) of glucose)) (Jung and Kim, 2017).

2.3. The LCNFs production and characterization

The solid fraction separated after the enzymatic hydrolysis was fibrillated for LCNFs production at 1% solids loading using a high-speed blender (TNC5200, Vitamix, Cleveland, OH, USA) at 37 000 r/min for 0–240 min. Sedimentation tests using gravitational force were conducted to indirectly evaluate the dispersibility of LCNFs. A 0.4% aqueous suspension (10 mL) of LCNFs was mixed using a vortex mixer for 10 s and maintained at room temperature (RT) without shaking for 48 h. The sedimentation ratio was expressed as a percentage of the height of the sedimentation layer over time (H_s) and the initial height (H_o) (Jang et al., 2021).

The morphological characteristics of the produced LCNFs were examined by field-emission scanning electron microscopy (FE-SEM; SU8030, Hitachi, Tokyo, Japan). A drop of the LCNFs suspension was dried at RT for 12 h on an aluminum foil and sputter-coated with osmium after mounting on a substrate with carbon tape to enhance conductivity. All images were captured at an accelerating voltage of 3 kV.

The chemical structure of the LCNFs dried in an oven at 40°C for 24 h was determined by Fourier-transform infrared (FT-IR) spectrophotometry (Nicolet iS5, Thermo Fisher Scientific, Waltham, MA, USA) using an attenuated total reflectance accessory (iD7, Thermo Fisher Scientific) and a zinc selenide crystal. The FT-IR spectra were acquired using the OMNIC 9 software (OMNIC version 9.7.46, Thermo Fisher Scientific) in the transmission mode in the range of 4 000–550 cm^{-1}. The spectra were recorded at a resolution of 4 cm^{-1} with 16 scans. External effects on the spectra were excluded by performing background correction.

2.4. Preparation and characterization of chitosan-based composite films

Chitosan (viscosity, 9.8 cPs; deacetylation degree, 95.44%) was supplied by Sokcho Corporation (Sokcho, Gangwon-do, Korea). Chitosan-LCNFs composite films were produced by using the modified method of Crouvisier-Urion et al. (2016) based on the solvent casting method. Briefly, a 1% chitosan solution was prepared by dissolving chitosan in 1% (*w/w*) acetic acid at 350 r/min for 4 h at RT. An LCNFs suspension (1% solids loading) was added to the completely dissolved chitosan solution at ratios of 1:1, 1:3, and 1:9 (*V/V*), and the mixture was vigorously stirred for 12 h at 350 r/min. The mixture was then poured into a polystyrene dish (9 cm × 9 cm) and dried at ambient temperature.

The mechanical properties of the LCNF-containing films, such as tensile strength, Young's modulus, and elongation at break, were determined using a universal testing machine (UTM; Zwick/Roell Z010, Zwick, Ulm, Germany) equipped with a 500-N load cell. The test specimens were cut into rectangular shapes with dimensions of 1 cm × 6 cm, and the thickness of each film was previously measured using a micrometer (IP65, Mitutoyo, Kawasaki, Japan). The tests were performed with a grip-to-grip separation of 10 mm at the start position, a speed of 5 mm/min, and a preload of 0.1 N.

The optical properties of the LCNF-containing films were determined using an ultraviolet-visible (UV–Vis) spectrophotometer (EPOCH2, Biotek, Winooski, VT, USA) in the wavelength range of 300–900 nm. The opacity value was estimated as the ratio of Abs_{600} to *d*, where Abs_{600} and *d* (mm) indicate the absorbance at 600 nm and the thickness of the films, respectively (Behera et al., 2021).

2.5. Statistical analysis

The significance of differences between data was determined using a one-way analysis of variance with values of $P < 0.05$. Data were expressed as the mean ± standard deviation of three independent experiments.

3. Results and discussion

3.1. Effect of chemical pretreatment on rice husks

The initial composition of the rice husks was 30.88% (*w/w* on a dry-weight basis) glucan, 16.35% xylan, 25.27% acid-insoluble lignin, and 0.97% acid-soluble lignin (Fig. 1a). The remaining components (15%–28%) might be mineral components, such as silica (Ma'ruf et al., 2017). An acidic catalyst was initially used to remove hemicellulose, because acid treatment of lignocellulosic biomass at a high temperature (i.e., 190°C) generally causes complete hydrolysis of hemicellulose with partial digestion of cellulose (Jung and Kim, 2015). As expected, xylan was also not detected (data not shown) during the acidic hydrolysis at various temperatures. Therefore, the different contents of lignin in the remaining solids were selected by adjusting pretreatment times at 190°C. The rice husks were subjected to the acid pretreatment for 5, 20, and 60 min, with the three time points being designated as 5A, 20A, and 60A, respectively, at a fixed temperature of 190°C with 1% (*w/w*) sulfuric acid and 15% (*w/V*) solid loading. Only after 5 min of pretreatment, 100% removal of xylan (hemicellulose) was achieved (Fig. 1a). The solubilized hemicellulose, the primary component in the hydrolysate obtained after pretreatment (Fig. 1b), could also be valuable as a prebiotic (Hong et al., 2019) or for conversion into other chemical components such as hydroxymethylfurfural (HMF), furfural, levulinic acid, and ethanol (Bhatia et al., 2021).

After 5 min of acid pretreatment, the rice husk (5AS) primarily consisted of ~41.6% glucan and 36.7% lignin (Fig. 1a). As the pretreatment progressed from 5 to 60 min, the residual glucan content decreased to 24.1% as the total lignin content increased to 57.0%. Considering the initial amounts of glucan and lignin, the glucose recovery yields markedly decreased from 78.5% to 33.5%;

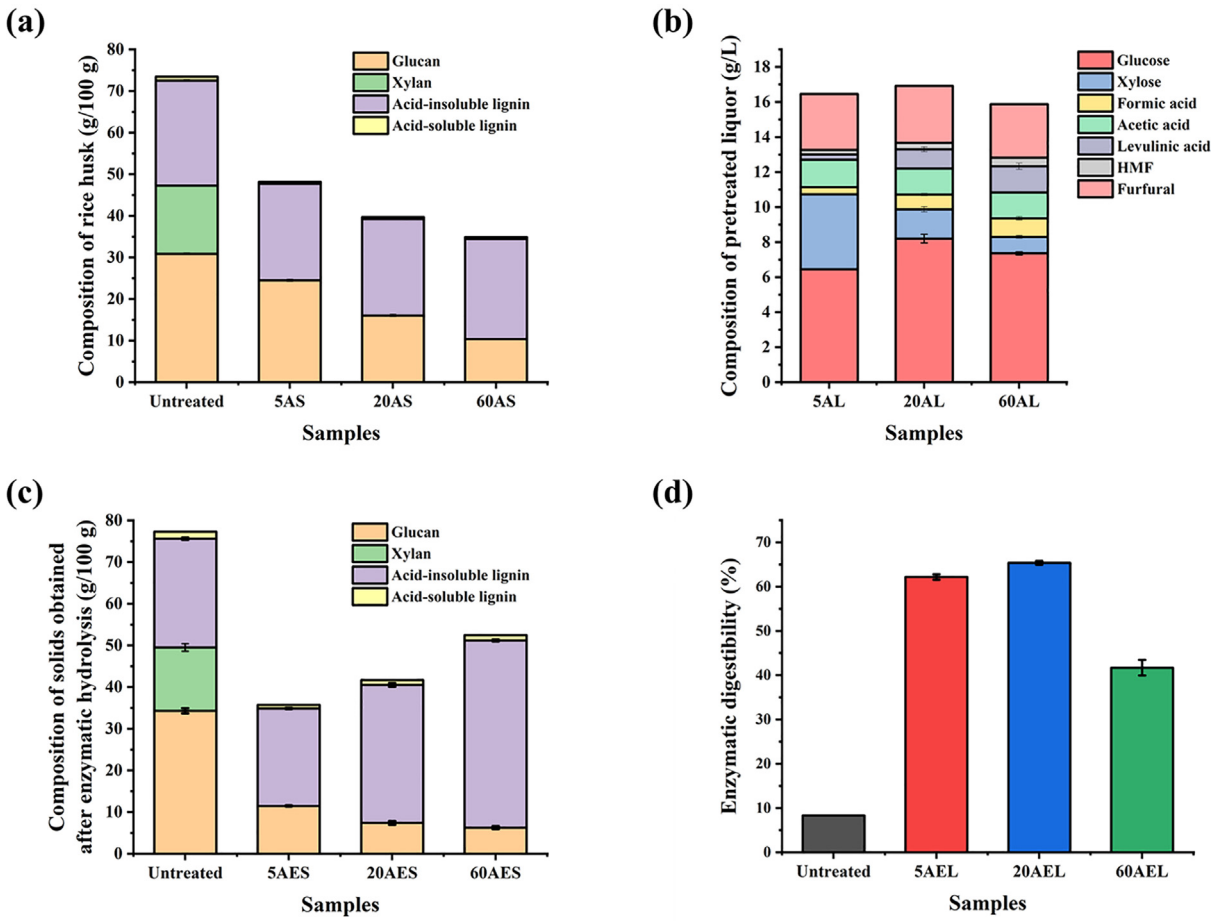

Fig. 1. Composition of untreated and pretreated rice husk in (a) solid fraction and (b) liquid fraction and (c) compositions of solids obtained after enzymatic hydrolysis and (d) enzymatic digestibility with 20 FPU of enzyme/glucan for 48 h at 50°C after chemical pretreatment for various times. 5AS, 20AS, and 60AS are the solid fractions obtained after acidic pretreatment for 5, 20, and 60 min; 5AL, 20AL, and 60AL are the liquid fractions obtained from acidic pretreatment for 5, 20, and 60 min; 5AES, 20AES, and 60AES are the solid fractions obtained after acidic pretreatment and enzymatic hydrolysis sequentially; 5AEL, 20AEL, and 60AEL are the liquid fractions obtained after acidic and enzymatic hydrolysis.

however, the lignin solids were enriched after pretreatment (i.e., 81.5%–93.4%) (Fig. 1a). These data show that solids with different lignin contents can be obtained by controlling the acid pretreatment time. Because the cellulose-rich biomass solids can be a source of fermentable sugars, such as glucose (Jung et al., 2013), and the lignin-rich biomass solids can be a source of biocomposite films (Liu et al., 2021), the appropriate pretreatment time can be modified based on the specific purpose.

As a next step, the cellulose in the acid-pretreated rice husk was hydrolyzed with 20 FPU of cellulase per gram glucan for 48 h at 50°C (Figs. 1c and 1d). Consequently, the solubilization degree of glucose reached 62.18% with biomass pretreated for 5 min (5AEL) and 65.38% with 20AEL in contrast to a maximum of 8.32% from the untreated rice husk control (Fig. 1d). However, the solubilization degree of glucose for sample 60AEL significantly decreased (41.68% glucose), probably due to the reduction in enzymatic digestibility under the extended acidic conditions (Kim et al., 2019). The high proportion of lignin in sample 60AS (Fig. 1a**)** might also negatively affect the enzyme activities or accessibilities of pretreated solids through lignin-enzyme interactions (Kellock et al., 2019; Yoo et al., 2020).

Overall, the glucan content in rice husks significantly reduced from 30.88% to a minimum of 9.07% after both acidic pretreatment and enzymatic hydrolysis, and the lignin content significantly increased from 26.24% to a maximum of 66.76%. This change in the proportion of structural components was subsequently investigated for their compatibility with LCNFs.

3.2. The LCNFs production from lignin-rich rice husk and its characterization

The three rice husk samples resulting after pretreatment and enzymatic hydrolysis (5AES, 20AES, and 60AES) were fibrillated using a high-speed blender to enhance the surface internetwork properties and stabilities of LCNFs (Ehman et al., 2020; Silva et al., 2021), which were evaluated using sedimentation test, FT-IR, and SEM **(**Fig. 2**)**. The LCNFs produced using 5AES, 20AES, and 60AES samples were designated as LCNF5, LCNF20, and LCNF60, respectively. The sedimentation ratio (H_s/H_o) considerably increased with

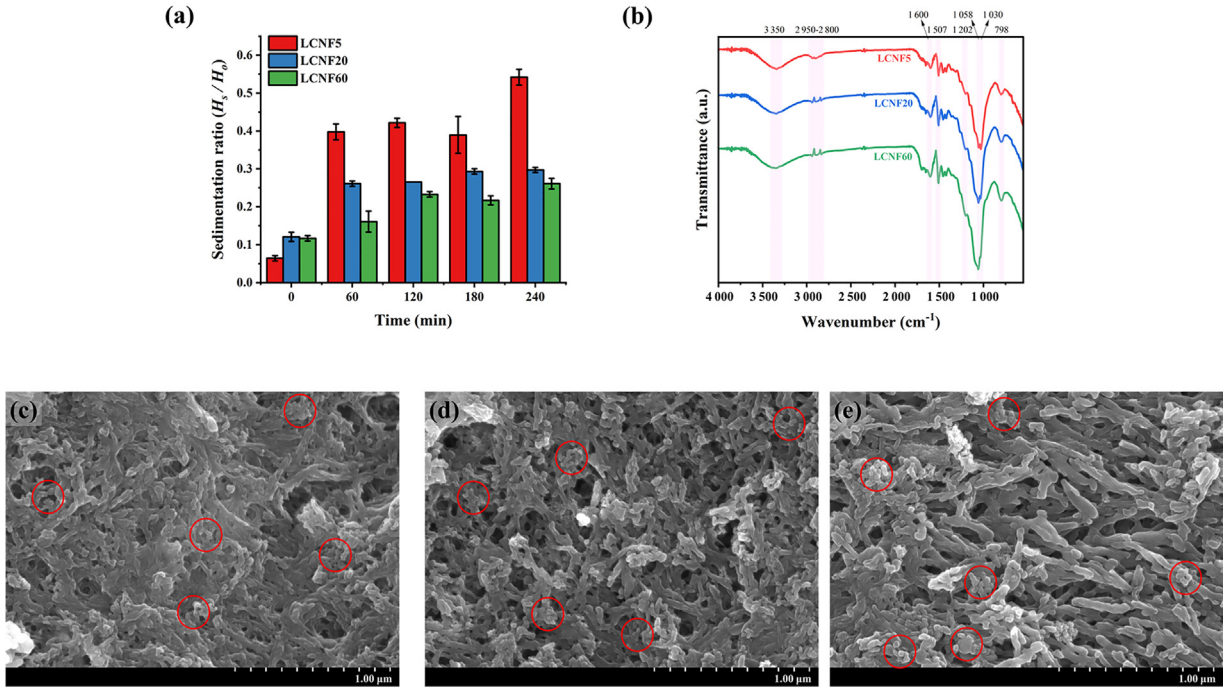

Fig. 2. (a) Effect of different grinding times on sedimentation of lignocellulosic nanofibers (LCNFs) from pretreated and enzymatically hydrolyzed rice husks, (b) Fourier transform infrared (FT-IR) spectra of LCNF5, LCNF20, and LCNF60 in the spectral range of 4 000–550 cm^{-1}, and scanning electron microscope (SEM) images of (c) LCNF5, (d) LCNF20, and (e) LCNF60 (lignin marked red circles in SEM images).

the initial treatment, but the extent of increase differed according to the pretreatment time (Fig. 2a). Specifically, the H_s/H_o ratio of LCNF5 increased from 0.06 to 0.40 after 60 min of blending and further increased to a maximum of 0.54 at 240 min of blending, which is equivalent to an 8.44-fold increase. The LCNF20 and LCNF60 also demonstrated comparable tendencies in the sedimentation ratio; however, with continuous fibrillation, the enhancement of the sedimentation ratio was not significant, which was probably affected by the low glucan content. Irrespective of cellulose and lignin contents, sufficient fibrillations occurred with initial blending.

The FT-IR spectroscopy revealed the presence of typical cellulose and lignin spectra without distinct structural alterations in the LCNFs irrespective of pretreatment because no chemical reaction was performed during high-speed blending, as reported previously (Chen et al., 2018; Han et al., 2020). Briefly, the identified spectra (Fig. 2b) were at 3 350 cm^{-1} (for O–H stretching) (Chen et al., 2018), 2 950–2 800 cm^{-1} (for C–H stretching vibration) (Jang et al., 2021), 1 058 cm^{-1} (for C–O–C pyranose ring skeletal vibration) (Jiang and Hsieh, 2016), and 1 030 cm^{-1} (for C–O, C=C, and C–C by cellulose and lignin) (Lazzari et al., 2019). Furthermore, from the absorption band at 798 cm^{-1} corresponding to Si–O–Si vibrations from silica (Ludueña et al., 2011), no structural changes were observed in the silica (Das and Goud, 2021). This finding also suggests that the remaining silica could act as an inorganic composite filler for the produced LCNFs without any other additional process. Remarkable increases in peaks at 1 600 cm^{-1} and 1 507 cm^{-1} (for aromatic phenyl (C=C) by lignin) and 1 202 cm^{-1} (for C–O bending vibration) (Zhang et al., 2019) were consistent with the result of compositional analysis (Fig. 1).

In Figs. 2c–2e, the SEM images demonstrated that large amounts of spherical particles were attached to the fiber surface and the abundance of spherical particles (lignin marked red circles in SEM images) indicates a high content of lignin in the solids (Herzele et al., 2016; Chen et al., 2018). However, the fiber boundaries were not observed clearly because of the aggregation of lignin spheres in and around the channels between the fibers and lignin (Chen et al., 2018; Jung et al., 2021; Xu et al., 2021) and in LCNF20 and LCNF60, which have a relatively low glucan content, and numerous pores were observed instead of agglomerates.

3.3. Preparation of chitosan-based LCNF films and their characterization

The surface morphologies of the prepared LCNFs were evaluated after their incorporation into chitosan films (Fig. 3). The pure chitosan film (Fig. 3a) displayed a smooth, nonporous, and uniform morphology, as observed in previous studies (Qiu et al., 2014; Behera et al., 2021). However, with 3 kV of accelerating voltage, the electron beam rendered the pure chitosan film unstable and induced surface cracks (Merz, 2019). The chitosan-LCNF5 composite films with contents in the range of 0%–50% (10% of LCNFs content, 5.06% lignin in the matrix; 25%, 12.65%; 50%, 25.30%) exhibited good dispersion of LCNFs in the chitosan matrix. Moreover, the surface roughness of the films increased with an increase in the LCNFs content (Figs. 2c–2e and 3a-3d). All LCNF particles, including LCNF5, LCNF20, and LCNF60, were well dispersed through the chitosan matrix and covered the surfaces. Furthermore, the

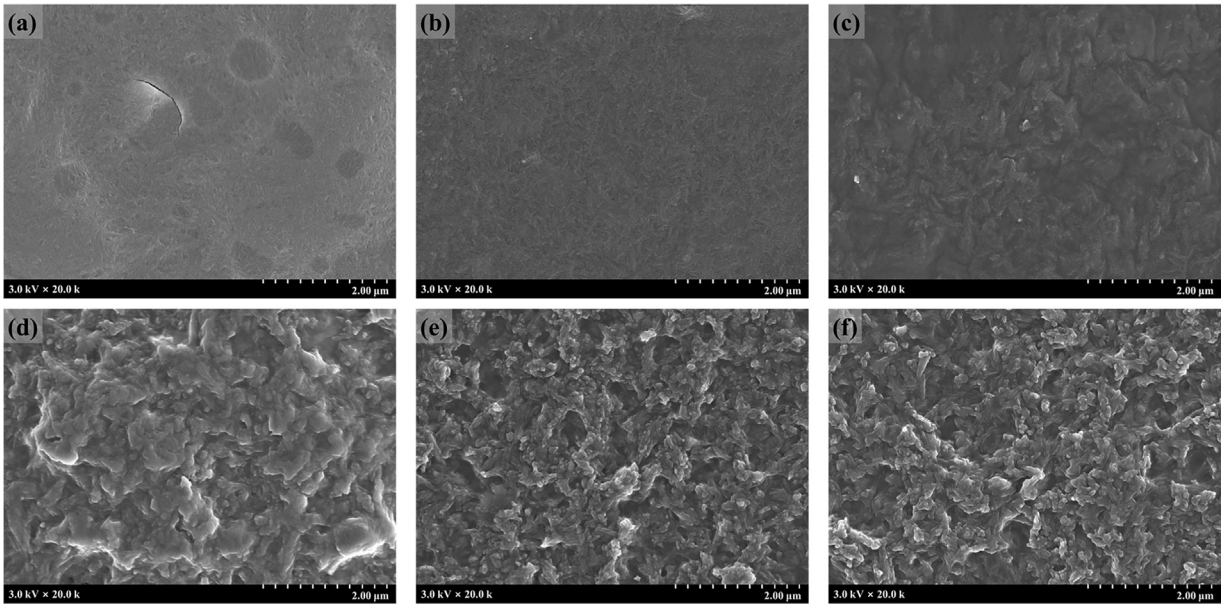

Fig. 3. The SEM images of chitosan-LCNF films: (a) pure chitosan film; (b) chitosan: LCNF5 (9:1, *V:V*) film; (c) chitosan:LCNF5 (3:1, *V:V*) film; (d) chitosan:LCNF5 (1:1, *V:V*) film; (e) chitosan:LCNF20 (1:1, *V:V*) film; and (f) chitosan: LCNF60 (1:1, *V:V*) film.

abovementioned instability of the 100% chitosan film caused by the irradiation treatment improved with the addition of LCNFs, and no cracks were observed after extended beam irradiation times during measurement (Figs. 3b–3d).

The dispersion of LCNFs in chitosan was reconfirmed by FT-IR spectroscopic analysis after incorporation into the films (Fig. 4). The composites showed that the spectra at 3 400–3 200 cm^{-1} and 3 000–2 800 cm^{-1} were attributed to O–H and N–H stretching and C–H stretching vibrations, respectively (Martins et al., 2012). The chitosan-based film also displayed specific peaks, such as those at 1 537, 1 404, and 1 019 cm^{-1}, which are associated with NH_2 bending, C–H bending of the CH_2 bond (Terzioglu et al., 2020), and symmetric stretching of the C–O–C bond (Ibrahim et al., 2022), respectively. With the addition of LCNFs, these peaks assigned to chitosan decrease since the relative ratio of chitosan decreases as the total weight of composites. Furthermore, the strong peak near 1 019 cm^{-1} is the result of an overlap of the C–O stretch of chitosan and the C–O–C pyranose ring skeletal vibration of LCNFs (Ji et al., 2022). The peak at 785 cm^{-1}, corresponding to the Si–O–Si bond of the rice husk-derived LCNFs, became stronger with an increase in the LCNFs content. These changes in the spectrum indicated proper dispersion of LCNFs in the chitosan.

3.4. Optical and mechanical properties of chitosan-based LCNF films

As a barrier to UV and visible light, optical properties comprise one of the most important key factors for packaging materials. In particular, in the food sector, UV lights catalyze oxidation and chemical reactions, which is a factor that decreases the quality of food (Hamdi et al., 2019). The optical properties of chitosan-based LCNF composite films were evaluated using an UV-Vis spectrophotometer (Table 1), where the transmittance values at 300 and 350 nm represent the UV light region, and the values at 450, 550, and 650 nm represent the visible light region. Compared with the transmittance of the 100% chitosan film as a control, the opacity of the films significantly increased with increasing LCNF concentrations, which caused a reduction in transmittance over the entire wavelength range. At a mixing ratio of 1:1, the chitosan-LCNF composite films demonstrated high UV-blocking capacity. When

Table 1
Optical transmittance and opacity of chitosan-LCNF composite films.

Sample	Ratio (*V:V*)	Transmittance (%)					Opacity
		300 nm	350 nm	450 nm	550 nm	650 nm	
Chitosan	–	6.30 ± 1.21^{a,*}	19.81 ± 2.49^{a}	76.97 ± 0.54^{a}	89.61 ± 0.24^{a}	91.55 ± 0.32^{a}	1.04 ± 0.12^{d}
Chitosan-LCNF5	9:1	0.00 ± 0.00^{b}	0.02 ± 0.00^{b}	13.41 ± 1.40^{b}	38.34 ± 1.90^{b}	56.08 ± 1.58^{b}	3.04 ± 0.06^{d}
	3:1	0.00 ± 0.00^{b}	0.00 ± 0.00^{b}	3.02 ± 0.48^{c}	17.13 ± 1.27^{c}	33.45 ± 1.60^{c}	7.45 ± 0.69^{cd}
	1:1	0.00 ± 0.00^{b}	0.00 ± 0.00^{b}	0.30 ± 0.10^{d}	5.21 ± 0.15^{d}	16.60 ± 1.49^{d}	16.62 ± 1.33^{c}
Chitosan-LCNF20	1:1	0.00 ± 0.00^{b}	0.00 ± 0.00^{b}	0.00 ± 0.00^{d}	0.19 ± 0.13^{e}	1.90 ± 1.11^{e}	40.04 ± 12.12^{b}
Chitosan-LCNF60	1:1	0.00 ± 0.00^{b}	0.00 ± 0.00^{b}	0.00 ± 0.00^{d}	0.00 ± 0.00^{e}	0.24 ± 0.07^{e}	54.34 ± 12.09^{a}

* Means values with different letters in the same column are significantly different according to Duncan's multiple range test by one-way ANOVA ($P < 0.05$). LCNF, lignocellulosic nanofiber.

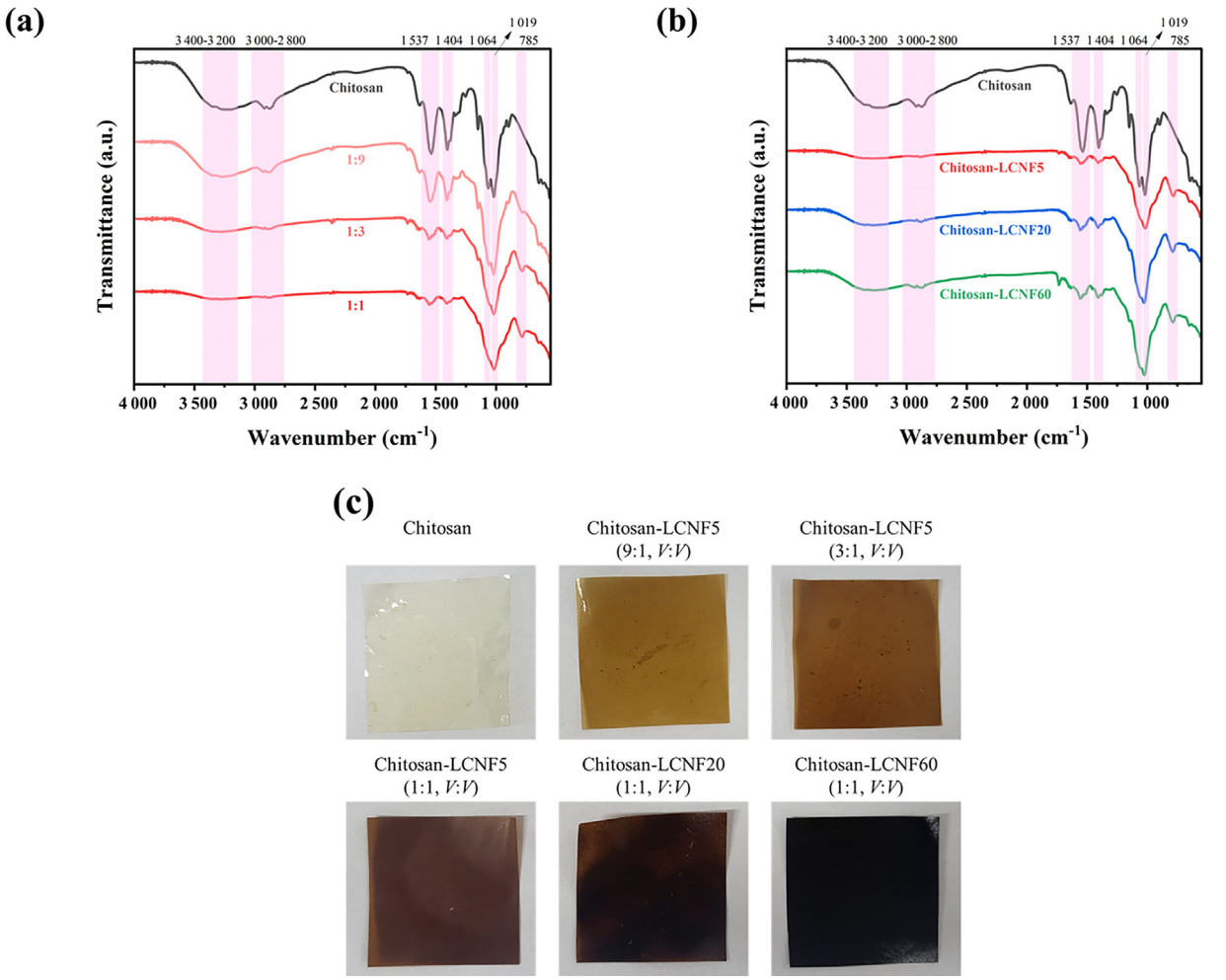

Fig. 4. The FT-IR spectra of chitosan-LCNF composite films (a) with various mixing ratios of chitosan:LCNF (9:1, 3:1, and 1:1, *V:V*) and (b) using LCNFs with different chemical pretreatment times in the spectral range of 4 000–550 cm^{-1} and (c) photographs of chitosan-LCNF composite films.

mixed with LCNF60, the films displayed their lowest transmittance. Moreover, with an increase in the lignin content, the film colors became darker (Fig. 4c), resulting in a stronger blocking effect of UV and visible light (Sadeghifar et al., 2017; Haqiqi et al., 2021). Accordingly, the opacity of the composite films increased from 16.62% to 54.34% with an increase in the pretreatment time, with the opacity being 52.25 times higher for chitosan-LCNF60 than for chitosan alone. Compared with pure chitosan films, LCNF-incorporated films can be a protective option for food deterioration. The desired opacity can be achieved by controlling the pretreatment time and adjusting the mixing ratio.

The mechanical properties of chitosan-based films were evaluated using an UTM (Fig. 5), which revealed a tensile strength of 48.6 MPa, an elongation of 41.0%, and Young's modulus of 153.5 MPa. The incorporation of LCNFs resulted in a noticeable elevation in Young's modulus for all composite films when compared to the pure chitosan film. Young's modulus serves as an indicator of film rigidity. This enhancement is ascribed to the inherent characteristics of LCNFs and the robust bonds established between chitosan and LCNFs. These strong intermolecular connections play a pivotal role in facilitating an effective transfer of loads from the matrix to the reinforcement (Elhussieny et al., 2020). Also, with various mixing ratios of chitosan:LCNF5, the mechanical properties of the composite film decreased with increasing LCNF content. The use of LCNFs as fillers in composite films is expected to improve the mechanical properties of the films (Trifol et al., 2021). However, at higher filler loading, the lack of uniform dispersion and aggregation of lignin could result in uneven stress transfer between lignin and the matrix polymer. Consequently, an appropriate amount of LCNF input is required compared with the solvent (Chen et al., 2009; Shankar et al., 2015). In contrast, LCNF60 exhibited higher tensile strength and higher elongation at break than LCNF5 and LCNF20 mixed at 1:1 ratio (Figs. 5a and 5b), which could be due to improved compatibility between lignin and the chitosan composite matrix. This could be attributed to the porous structure of LCNFs observed in SEM images (Figs. 2c–2e), which enables improvement of compatibility in the composite matrix. Previous studies have reported that a porous structure on the surface of lignin improves the tensile strength in the composite biopolymers of lignin and agar by forming strong hydrogen bonds (Chen et al., 2009; Korbag and Mohamed Saleh, 2016). Hence, the mechanical properties

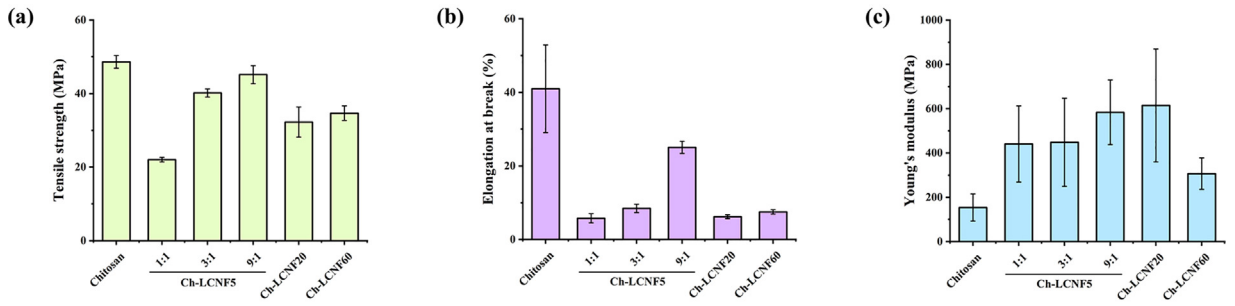

Fig. 5. (a) Tensile strength, (b) elongation at break, and (c) Young's modulus of chitosan-LCNF composite films. Ch-LCNF5, Ch-LCNF20, and Ch-LCNF60 are the composite films of chitosan and LCNF5, LCNF20, and LCNF60, respectively.

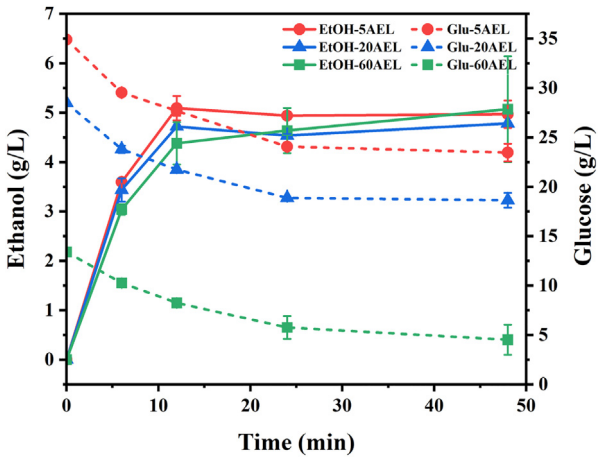

Fig. 6. Ethanol production capacity of hydrolysates recovered from enzymatic hydrolysis after pretreatment. EtOH-5AEL, EtOH-20AEL, and EtOH-60AEL are the ethanol concentration in the fermentation process using 5AEL, 20AEL, and 60AEL; Glu-5AEL, Glu-20AEL, and Glu-60AEL are the glucose concentration in the fermentation process using 5AEL, 20AEL, and 60AEL.

of chitosan-based composite films could be further optimized by adjusting the solid loading and pretreatment time or by adding a plasticizer. Moreover, although LCNFs addition (about 10%) showed film-forming ability under chitosan structure, the film properties may vary depending on the LCNFs properties and LCNFs amounts, it is necessary to apply it by considering the physical properties desired by the user (e.g., tensile or optical properties).

3.5. Ethanol production using soluble fractions obtained after enzymatic hydrolysis

As a further study of LCNFs production using residual solids obtained from enzymatic hydrolysis, the glucose solutions in the liquor fraction obtained after hydrolysis were used as substrates for ethanol fermentation to demonstrate the feasibility of using rice husk as a raw material in the biorefinery industry. The soluble glucose solutions were used as a sugar source for fermentation by *S. cerevisiae* D_5A (Fig. 6). The fermentation media contained 34.91 g/L (5AEL), 28.49 g/L (20AEL), and 13.41 g/L (60AEL) of glucose after the addition of YP medium to the soluble fractions. Both samples, 5AEL and 20AEL, have similar digestibility (62.18% and 65.38%), respectively (Fig. 1d); however, the initial glucose concentrations in fermentation media are different. This is because the input pretreated solids have different glucan concentrations (46.69% and 36.36%, respectively). The maximum ethanol production from rice husks was 5.07 g/L from 60AEL after 48 h, which revealed that the theoretical maximum ethanol yield could be 111.56% based on the amounts of glucose consumed. After the enzymatic hydrolysis, not only glucose but also cellobiose could be present in the fermentation medium used for fermentation (Wang and Gao, 2023). However, in this study, the ethanol yield was only calculated on the basis of the added glucose amount as well as the glucose consumption was relatively smaller, the theoretical maximum ethanol yield exceeded 100%. Other pretreatment conditions, such as 5AEL and 20AEL, resulted in ethanol yields of 85% and 94.98%, respectively. A maximum of 2.74 g/L of ethanol was produced from 100 g of soluble fractions of pretreated and enzymatically hydrolyzed rice husks. Irrespective of the different pretreatment methods, the amounts of glucose consumed during 48 h of fermentation ranged from 8.89 to 11.44 g/L, and 67% of the glucose remained in the media (Table 1). High concentration of glucose could affect glucose consumption because high concentration in the fermentation media can cause hyperosmotic stress on the cells (Sengupta et al., 2022). The final product yields could be enhanced using metabolically improved organisms that might be tolerant to various inhibitory compounds, including aldehydes and organic acids.

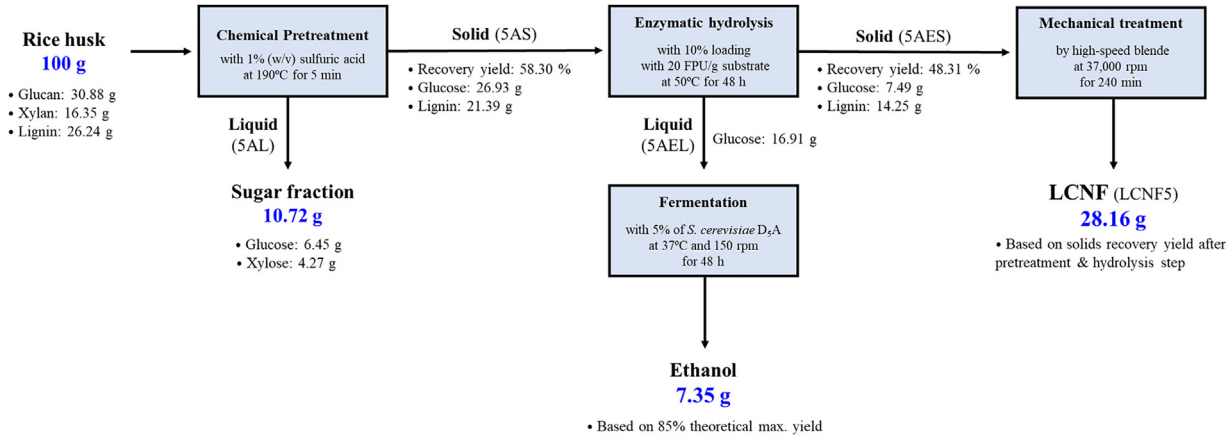

Fig. 7. Mass balance of overall process. *S.: Saccharomyces*.

The overall mass balance for the sequential production of sugar, ethanol, and LCNFs from the rice husk was calculated (Fig. 7). The flowchart shows the changes in the amount of the major components such as glucose, xylose, and lignin. First, after chemical pretreatment, the solid and liquor fractions contained 26.93 g of glucose and 10.7 g of sugars (glucose and xylose), respectively, from 100 g dry weight of rice husk. With subsequent saccharification and fermentation processes, 7.4 g of ethanol was obtained. The separated solids after enzymatic hydrolysis could be utilized in the production of LCNFs (28.2 g) with compositions of 7.49 g glucose and 14.25 g lignin. Either obtaining a high titer of ethanol production or a high amount of LCNFs production is essential for maintaining sustainability, and it is necessary to perform further targeted process optimization.

4. Conclusions

The LCNFs containing both cellulose and lignin were successfully obtained from rice husks after acidic pretreatment and enzymatic hydrolysis. Depending on the pretreatment conditions, different concentrations of lignin were obtained from the rice husk, which resulted in altered hydrophobic properties of LCNFs. The LCNFs demonstrated high potential as an additive in chitosan-based composites and exhibited adjusted mechanical properties, which were primarily attributed to the proportion of lignin resulting from the different pretreatment times. Furthermore, since different lignin concentrations in LCNFs and different addition LCNFs may vary the final properties of chitosan-based LCNF films, further process optimization is required. In conclusion, after acidic and enzymatic treatments of rice husks, successful LCNFs production and complexation with chitosan were achieved, and bioethanol production from the LCNFs was simultaneously demonstrated.

Declaration of competing interest

There are no conflicts to declare.

Acknowledgments

This work was supported by the Technology Development Program funded by the Ministry of SMEs and Startups (MSS, Korea) [S2978549]. This work was also supported by the National Research Foundation of Korea (NRF) grant funded by Korea government (Ministry of Science and ICT, MSIT; No. 2020R1C1C1005251).

References

Banerjee, S., Sen, R., Pandey, R.A., Chakrabarti, T., Satpute, D., Giri, B.S., Mudliar, S., 2009. Evaluation of wet air oxidation as a pretreatment strategy for bioethanol production from rice husk and process optimization. Biomass Bioenergy 33, 1680–1686.

Behera, K., Kumari, M., Chang, Y.H., Chiu, F.C., 2021. Chitosan/boron nitride nanobiocomposite films with improved properties for active food packaging applications. Int. J. Biol. Macromol. 186, 135–144.

Bhatia, S.K., Jagtap, S.S., Bedekar, A.A., Bhatia, R.K., Rajendran, K., Pugazhendhi, A., Rao, C.V., Atabani, A.E., Kumar, G., Yang, Y.H., 2021. Renewable biohydrogen production from lignocellulosic biomass using fermentation and integration of systems with other energy generation technologies. Sci. Total Environ. 765, 144429.

Bian, H.Y., Chen, L.H., Dai, H.Q., Zhu, J.Y., 2017. Integrated production of lignin containing cellulose nanocrystals (LCNC) and nanofibrils (LCNF) using an easily recyclable di-carboxylic acid. Carbohydr. Polym. 167, 167–176.

Chen, L., Tang, C.Y., Ning, N.Y., Wang, C.Y., Fu, Q., Zhang, Q., 2009. Preparation and properties of chitosan/lignin composite films. Chin. J. Polym. Sci. 27, 739.

Chen, Y., Fan, D.B., Han, Y.M., Lyu, S.Y., Lu, Y., Li, G.Y., Jiang, F., Wang, S.Q., 2018. Effect of high residual lignin on the properties of cellulose nanofibrils/films. Cellulose 25, 6421–6431.

Cherubini, F., 2010. The biorefinery concept: using biomass instead of oil for producing energy and chemicals. Energy. Convers. Manag. 51, 1412–1421.

Chieng, S., Kuan, S.H., 2022. Harnessing bioenergy and high value–added products from rice residues: a review. Biomass Convers. Biorefin. 12, 3547–3571.

Crouvisier-Urion, K., Bodart, P.R., Winckler, P., Raya, J., Gougeon, R.D., Cayot, P., Domenek, S., Debeaufort, F., Karbowiak, T., 2016. Biobased composite films from chitosan and lignin: antioxidant activity related to structure and moisture. ACS Sustainable Chem. Eng. 4, 6371–6381.

Dagnino, E.P., Felissia, F.E., Chamorro, E., Area, M.C., 2017. Optimization of the soda-ethanol delignification stage for a rice husk biorefinery. Ind. Crops Prod. 97, 156–165.
Das, S., Goud, V.V., 2021. RSM-optimised slow pyrolysis of rice husk for bio-oil production and its upgradation. Energy 225, 120161.
Ehman, N.V., Lourenço, A.F., McDonagh, B.H., Vallejos, M.E., Felissia, F.E., Ferreira, P.J.T., Chinga-Carrasco, G., Area, M.C., 2020. Influence of initial chemical composition and characteristics of pulps on the production and properties of lignocellulosic nanofibers. Int. J. Biol. Macromol. 143, 453–461.
Elhussieny, A., Faisal, M., D'Angelo, G., Aboulkhair, N.T., Everitt, N.M., Fahim, I.S., 2020. Valorisation of shrimp and rice straw waste into food packaging applications. Ain Shams Eng. J. 11, 1219–1226.
Fernandes, S.C.M., Freire, C.S.R., Silvestre, A.J.D., Pascoal Neto, C., Gandini, A., Berglund, L.A., Salmén, L., 2010. Transparent chitosan films reinforced with a high content of nanofibrillated cellulose. Carbohydr. Polym. 81, 394–401.
Hamdi, M., Nasri, R., Li, S.M., Nasri, M., 2019. Bioactive composite films with chitosan and carotenoproteins extract from blue crab shells: biological potential and structural, thermal, and mechanical characterization. Food Hydrocoll. 89, 802–812.
Han, X.S., Bi, R., Oguzlu, H., Takada, M., Jiang, J.G., Jiang, F., Bao, J., Saddler, J.N., 2020. Potential to produce sugars and lignin-containing cellulose nanofibrils from enzymatically hydrolyzed chemi-thermomechanical pulps. ACS Sustainable Chem. Eng. 8, 14955–14963.
Haqiqi, M.T., Bankeeree, W., Lotrakul, P., Pattananuwat, P., Punnapayak, H., Ramadhan, R., Kobayashi, T., Amirta, R., Prasongsuk, S., 2021. Antioxidant and UV-blocking properties of a carboxymethyl cellulose-lignin composite film produced from oil palm empty fruit bunch. ACS Omega 6, 9653–9666.
Herzele, S., Veigel, S., Liebner, F., Zimmermann, T., Gindl-Altmutter, W., 2016. Reinforcement of polycaprolactone with microfibrillated lignocellulose. Ind. Crops Prod. 93, 302–308.
Hong, C., Corbett, D., Venditti, R., Jameel, H., Park, S., 2019. Xylooligosaccharides as prebiotics from biomass autohydrolyzate. LWT 111, 703–710.
Howard, R.L., Abotsi, E., Jansen, V.R.E.L., Howard, S., 2003. Lignocellulose biotechnology: issues of bioconversion and enzyme production. Afr. J. Biotechnol. 2, 602–619.
Ibrahim, N.H., Iqbal, A., Mohammad-Noor, N., Razali, R.M., Sreekantan, S., Yanto, D.H.Y., Mahadi, A.H., Wilson, L.D., 2022. Photocatalytic remediation of harmful *Alexandrium minutum* bloom using hybrid chitosan-modified TiO_2 films in seawater: a lab-based study. Catalysts 12, 707.
Jang, J.H., Kang, H.J., Adedeji, O.E., Kim, G.Y., Lee, J.K., Kim, D.H., Jung, Y.H., 2023. Development of a pH indicator for monitoring the freshness of minced pork using a cellulose nanofiber. Food Chem. 403, 134366.
Jang, J.H., So, B.R., Yeo, H.J., Kang, H.J., Kim, M.J., Lee, J.J., Jung, S.K., Jung, Y.H., 2021. Preparation of cellulose microfibril (CMF) from *Gelidium amansii* and feasibility of CMF as a cosmetic ingredient. Carbohydr. Polym. 257, 117569.
Ji, M.C., Li, J.Y., Li, F.Y., Wang, X.J., Man, J., Li, J.F., Zhang, C.W., Peng, S.X., 2022. A biodegradable chitosan-based composite film reinforced by ramie fibre and lignin for food packaging. Carbohydr. Polym. 281, 119078.
Jiang, F., Hsieh, Y.L., 2016. Self-assembling of TEMPO oxidized cellulose nanofibrils as affected by protonation of surface carboxyls and drying methods. ACS Sustainable Chem. Eng. 4, 1041–1049.
Jiang, Y., Liu, X.Y., Yang, Q., Song, X.P., Qin, C.R., Wang, S.F., Li, K.C., 2018. Effects of residual lignin on mechanical defibrillation process of cellulosic fiber for producing lignocellulose nanofibrils. Cellulose 25, 6479–6494.
Jung, H., Kwak, H., Chun, J., Oh, K., 2021. Alkaline fractionation and subsequent production of nano-structured silica and cellulose nano-fibrils for the comprehensive utilization of rice husk. Sustainability 13, 1951.
Jung, Y.H., Kim, K.H., 2015. Acidic pretreatment. In: Pandey, A., Negi, S., Binod, P., Larroche, C. (Eds.), Pretreatment of Biomass: Process and Technologies. Academic Press, Cambridge, pp. 27–50.
Jung, Y.H., Kim, I.J., Kim, H.K., Kim, K.H., 2013. Dilute acid pretreatment of lignocellulose for whole slurry ethanol fermentation. Bioresour. Technol. 132, 109–114.
Jung, Y.H., Kim, K.H., 2017. Evaluation of the main inhibitors from lignocellulose pretreatment for enzymatic hydrolysis and yeast fermentation. Bioresources 12, 9348–9356.
Kellock, M., Maaheimo, H., Marjamaa, K., Rahikainen, J., Zhang, H., Holopainen-Mantila, U., Ralph, J., Tamminen, T., Felby, C., Kruus, K., 2019. Effect of hydrothermal pretreatment severity on lignin inhibition in enzymatic hydrolysis. Bioresour. Technol. 280, 303–312.
Kim, D.H., Park, H.M., Jung, Y.H., Sukyai, P., Kim, K.H., 2019. Pretreatment and enzymatic saccharification of oak at high solids loadings to obtain high titers and high yields of sugars. Bioresour. Technol. 284, 391–397.
Korbag, I., Mohamed Saleh, S., 2016. Studies on mechanical and biodegradability properties of PVA/lignin blend films. Int. J. Environ. Stud. 73, 18–24.
Lazzari, L.K., Zimmermann, M.V.G., Perondi, D., Zampieri, V.B., Zattera, A.J., Santana, R.M.C., 2019. Production of carbon foams from rice husk. Mat. Res. 22, e20190034. doi:10.1590/1980-5373-MR-2019-0427.
Liu, K., Du, H.S., Zheng, T., Liu, W., Zhang, M., Liu, H.Y., Zhang, X.Y., Si, C.L., 2021. Lignin-containing cellulose nanomaterials: preparation and applications. Green Chem. 23, 9723–9746.
Ludueña, L., Fasce, D., Alvarez, V.A., Stefani, P.M., 2011. Nanocellulose from rice husk following alkaline treatment to remove silica. Bioresources 6, 1440–1453.
Ma'ruf, A., Pramudono, B., Aryanti, N., 2017. Lignin isolation process from rice husk by alkaline hydrogen peroxide: lignin and silica extracted. In: AIP Conference Proceedings. Las Vegas, Nevada, USA.
Martins, J.T., Cerqueira, M.A., Vicente, A.A., 2012. Influence of α-tocopherol on physicochemical properties of chitosan-based films. Food Hydrocoll. 27, 220–227.
Merz, C.R., 2019. Physicochemical and colligative investigation of α (shrimp shell)- and β (squid pen)-chitosan membranes: concentration-gradient-driven water flux and ion transport for salinity gradient power and separation process operations. ACS Omega 4, 21027–21040.
Qiu, Y.F., Ma, Z., Hu, P.G., 2014. Environmentally benign magnetic chitosan/Fe_3O_4 composites as reductant and stabilizer for anchoring Au NPs and their catalytic reduction of 4-nitrophenol. J. Mater. Chem. A 2, 13471–13478.
Ranatunga, T.D., Jervis, J., Helm, R.F., McMillan, J.D., Hatzis, C., 1997. Toxicity of hardwood extractives toward *Saccharomyces cerevisiae* glucose fermentation. Biotechnol. Lett. 19, 1125–1127.
Rodionova, M.V., Bozieva, A.M., Zharmukhamedov, S.K., Leong, Y.K., Chi-Wei Lan, J., Veziroglu, A., Veziroglu, T.N., Tomo, T., Chang, J.S., Allakhverdiev, S.I., 2022. A comprehensive review on lignocellulosic biomass biorefinery for sustainable biofuel production. Int. J. Hydrog. Energy 47, 1481–1498.
Sadeghifar, H., Venditti, R., Jur, J., Gorga, R.E., Pawlak, J.J., 2017. Cellulose-lignin biodegradable and flexible UV protection film. ACS Sustainable Chem. Eng. 5, 625–631.
Sengupta, P., Mohan, R., Wheeldon, I., Kisailus, D., Wyman, C.E., Cai, C.M., 2022. Prospects of thermotolerant *Kluyveromyces marxianus* for high solids ethanol fermentation of lignocellulosic biomass. Biotechnol. Biofuels Bioprod. 15, 134.
Shaheen, S.M., Antoniadis, V., Shahid, M., Yang, Y., Abdelrahman, H., Zhang, T., Hassan, N.E.E., Bibi, I., Niazi, N.K., Younis, S.A., Almazroui, M., Tsang, Y.F., Sarmah, A.K., Kim, K.H., Rinklebe, J., 2022. Sustainable applications of rice feedstock in agro-environmental and construction sectors: a global perspective. Renew. Sustain. Energy Rev. 153, 111791.
Shankar, S., Reddy, J.P., Rhim, J.W., 2015. Effect of lignin on water vapor barrier, mechanical, and structural properties of agar/lignin composite films. Int. J. Biol. Macromol. 81, 267–273.
Silva, L.E., Dos Santos, A.A., Torres, L., McCaffrey, Z., Klamczynski, A., Glenn, G., Sena Neto, A.R., Wood, D., Williams, T., Orts, W., Damásio, R.A.P., Tonoli, G.H.D., 2021. Redispersion and structural change evaluation of dried microfibrillated cellulose. Carbohydr. Polym. 252, 117165.
Supanakorn, G., Varatkowpairote, N., Taokaew, S., Phisalaphong, M., 2021. Alginate as dispersing agent for compounding natural rubber with high loading microfibrillated cellulose. Polymers (Basel) 13, 468.
Terzioglu, P., Altin, Y., Kalemtas, A., Celik Bedeloglu, A., 2020. Graphene oxide and zinc oxide decorated chitosan nanocomposite biofilms for packaging applications. J. Polym. Eng. 40, 152–157.
Trifol, J., Marin Quintero, D.C., Moriana, R., 2021. Pine cone biorefinery: integral valorization of residual biomass into lignocellulose nanofibrils (LCNF)-reinforced composites for packaging. ACS Sustainable Chem. Eng. 9, 2180–2190.
Walls, L.E., Rios-Solis, L., 2020. Sustainable production of microbial isoprenoid derived advanced biojet fuels using different generation feedstocks: a review. Front. Bioeng. Biotechnol. 8, 599560.
Wang, Y., Gao, M., 2023. Efficient biorefinery based on designed lignocellulosic substrate for lactic acid production. Fermentation 9, 744.

Xu, R., Du, H.S., Wang, H., Zhang, M., Wu, M.Y., Liu, C., Yu, G., Zhang, X.Y., Si, C.L., Choi, S.E., Li, B., 2021. Valorization of enzymatic hydrolysis residues from corncob into lignin-containing cellulose nanofibrils and lignin nanoparticles. Front. Bioeng. Biotechnol. 9, 677963.

Yoo, C.G., Meng, X.Z., Pu, Y.Q., Ragauskas, A.J., 2020. The critical role of lignin in lignocellulosic biomass conversion and recent pretreatment strategies: a comprehensive review. Bioresour. Technol. 301, 122784.

Yousefhashemi, S.M., Khosravani, A., Yousefi, H., 2019. Isolation of lignocellulose nanofiber from recycled old corrugated container and its interaction with cationic starch–nanosilica combination to make paperboard. Cellulose 26, 7207–7221.

Zhang, L.L., Lu, H.L., Yu, J., McSporran, E., Khan, A., Fan, Y.M., Yang, Y.Q., Wang, Z.G., Ni, Y.H., 2019. Preparation of high-strength sustainable lignocellulose gels and their applications for antiultraviolet weathering and dye removal. ACS Sustainable Chem. Eng. 7, 2998–3009.

Zhu, J.Y., Sabo, R., Luo, X.L., 2011. Integrated production of nano-fibrillated cellulose and cellulosic biofuel (ethanol) by enzymatic fractionation of wood fibers. Green Chem. 13, 1339–1344.